Journal of Power Sources 247 (2014) 579–586

Contents lists available at ScienceDirect

Journal of Power Sources

journal homepage: www.elsevier.com/locate/jpowsour

Performance of non-compartmentalized enzymatic biofuel cell based on buckypaper cathode and ferrocene-containing redox polymer anode

Christine Bunte [a, 1], Laith Hussein [b, c, *, 1, 2], Gerald A. Urban [b, c]

[a] Department of Microsystems Engineering (IMTEK), Laboratory for Chemistry and Physics of Interfaces, University of Freiburg, Freiburg, Germany
[b] Freiburg Materials Research Centre (FMF), University of Freiburg, Freiburg, Germany
[c] Department of Microsystems Engineering (IMTEK), Laboratory for Sensors, University of Freiburg, Freiburg, Germany

HIGHLIGHTS

- Enzymatic single compartment glucose/O_2 fuel cells were developed.
- Buckypaper-based cathode and ferrocene-containing redox polymer-based anode were employed.
- The resulting biofuel cell generates an open circuit voltage of approximately 0.550 V.
- The peak power density in quiescent buffer containing 5 mM glucose approaches 26 μW cm^{-2}.

ARTICLE INFO

Article history:
Received 15 May 2013
Received in revised form
26 July 2013
Accepted 20 August 2013
Available online 11 September 2013

Keywords:
Biofuel cell
Glucose
Buckypaper
Redox polymer
Mediated electron transfer
Implantable power

ABSTRACT

Novel single compartment Glucose/O_2 biofuel cells (BFCs) were developed using immobilized enzymes and the mediated electron transfer (MET) approach. The bioanode was prepared through a ferrocene-containing redox polymer crosslinked in the presence of a biocatalyst on a glassy carbon support. Here, the redox polymer can physically entrap the enzyme and prevent it from leaching. Additionally it provides a biocompatible microenvironment and thus could extend the life time of enzyme. On the other side, the mediated biocathode was prepared based on bilirubin oxidase and 2,2′-azinobis(3-ethylbenzothiazoline-6-sulfonate) diammonium salt ($ABTS^{2-}$) system which has been physically entrapped in Nafion matrix and then adsorbed directly on a highly porous, conductive and functionalized buckypaper (fBP). Both electrodes were characterized physically and electrochemically. Employing these electrodes, the resulting BFC generates an open circuit voltage (V_{oc}) of approximately 0.550 V and a peak power density of 26 μW cm^{-2} at 0.2 V at 37 °C in quiescent O_2-saturated physiological buffer containing 5 mM glucose. The cell sustains a load up to 225 μA cm^{-2}. Moreover, a high short circuit current (I_{sc}) of 300 μA cm^{-2} is approached. This BFC can operate in mild conditions without using any toxic materials which makes it attractive for implantable devices.

1. Introduction

Many efforts have been devoted recently to enzymatic biofuel cells (BFCs) which convert available chemical free energy of biofuels (e.g. glucose or organic acids) directly into electrical energy. This process is coupled with the reduction of molecular oxygen by means of inexpensive enzymatic catalysts for at least one of these two reactions. It has been shown that certain enzymes possess highly favorable catalytic properties in comparison to inorganic catalysts. For example, Heller et al. have proposed that the multi-copper oxidases, e.g. laccase and bilirubin oxidase (BOD), are more efficient electrocatalysts than Pt for the four-electron oxygen

* Corresponding author. Department of Microsystems Engineering (IMTEK), Laboratory for Sensors, University of Freiburg, Freiburg, Germany. Fax: +49 7612 037262.
E-mail addresses: laith.hussein@fmf.uni-freiburg.de, hussein@ac.chemie.tu-darmstadt.de (L. Hussein).
[1] Both authors made equal contribution to this work and thus the order of authors is ranked alphabetically.
[2] Current address: Eduard-Zintl-Institute of Inorganic and Physical Chemistry, Darmstadt University of Technology, Darmstadt, Germany. Fax: +49 (0) 6151/163470.

0378-7753/$ – see front matter © 2013 Elsevier B.V. All rights reserved.
http://dx.doi.org/10.1016/j.jpowsour.2013.08.077

reduction reaction (ORR), as O_2 is reduced at a smaller overpotential on enzymatic than on platinum electrodes [1].

In addition some enzymes operate optimally in pH neutral aqueous media, making them attractive for implantable devices [2], [3]. In contrast to other batteries or fuel cells, enzymatic BFCs utilize renewable catalysts and fuels, and do not contain toxic or corrosive components. Moreover, they can be designed to operate in mild conditions.

Due to the unmatched selectivity of the anode and cathode, mixed-reactant fuel cells may be designed which do not show cross-reactions (cross-talk) and have comparable optimum environmental working conditions. Therefore, the BFCs can operate in a simple single compartment which facilitates an exceptional degree of miniaturization [3].

These features have motivated intense research efforts since the initiative work of Yahiro et al. in 1964 [4]. Yet, no commercial BFC has been launched to the present day [5]. Only very recently have the first prototypes been demonstrated [6,7], which could find applications in portable power sources. The main drawbacks that need to be tackled are the limited power output and short life time of the devices, mainly due to enzyme inactivation, leaching of active materials and other aspects such as impurities and contaminants [8,9]. The central challenge arises from the intrinsic properties of the biocatalysts. Making efficient and stable electrocatalysts is one of the most important goals in energy applications [9]. For high efficiency, the reaction has to be achieved at a substantial turnover frequency under thermodynamic conditions as close as possible to reversibility [10].

Although oxidoreductase enzymes with a turnover number on the order of 1000 s^{-1} are available, their large sizes lead to a total surface density of catalytic sites in the range of picomoles per square centimeter [8]. The limiting current densities of electrodes covered with a monolayer of biocatalysts are typically well below 100 μA cm^{-2} [8], which is too low for most applications. Accordingly, an important field of research is to develop strategies for high accessible surface area in order to simultaneously address multiple layers of the catalyst film. Micro- and nanostructured conductive materials are therefore used, including mesoporous carbon, silica matrixes, porous chitosan scaffolds composites, carboneous foams, carbon nanotubes [11–14], and metallic nanoparticles [15].

In such a context these three-dimensional matrices can be superior candidates for high enzyme loading and effective mass transport in the design of efficient BFCs and biosensors. This is because they produce a higher and more stable catalytic current than planar (flat) electrodes, with homogenous convection of glucose and dioxygen. For example, we recently reported that flexible, highly conductive and mesoporous buckypaper (i.e. a carbon nanotube mat) can be utilized to immobilize bilirubin oxidase (BOD), and can yield a high biocatalytic current density of up to 240 μA cm^{-2} in air-saturated physiological buffer [16]. All of these strategies require an efficient communication or direct electron transfer (DET) between the enzyme active center and the conductive support.

Also noteworthy is that true DET is often referred to as electron tunneling processes, and if intramolecular DET is too slow an artificial electronic wire is required. This concept of mediated electron-transfer (MET) relies on redox active units which have a potential closed to enzyme redox potential to “shuttle” electrons between the active site of the enzyme and the conductive support. Typical MET mediators are 2,2′-azinobis(3-ethylbenzothiazoline-6-sulfonate) diammonium salt ($ABTS^{2-}$) [17], quinone complexes and transition metal complexes such as ferrocene derivatives [17–20], ferricyanides, osmium or ruthenium complexes [21–24], which can be added as diffusing species to the electrolyte, or immobilized on the electrode surface [25–28].

Currently, four strategies of enzyme immobilization are usually employed, including physical adsorption, covalent binding, physical entrapment, and layer-by-layer self assembly. Perhaps the most successful immobilization strategy was suggested by Heller’s group, and relies on the covalent attachment of the mediator to the backbone of a crosslinked polymer. Such mediator units possess some mobility and can thus exchange electrons with the active centers of immobilized biocatalyst, and transport these electrons through a depth equivalent to hundreds of monolayers. A much larger number of enzymes can thus be electrically “wired” to the conductive support, irrespective of the orientation of the catalyst with respect to the electrode surface. Mostly osmium complexes are utilized as they can be “tuned” to cover a large potential window. However for implantable applications, the use of this type of redox mediator is questionable due to its potential negative health implications [29].

In this work, we present the assembly and electrochemical characterization of complete enzymatic BFCs, by combining the advantageous features of efficient and non-toxic mediated bioelectrocatalytic systems. The cells operate in a single compartment under physiological conditions and are highly promising for micropower sources. The results shown here are based on our previous work for glucose-oxidizing bioanodes and oxygen-reducing biocathodes [16,30–32], and were part of the PhD work of C. Bunte and L. Hussein [33,34].

2. Experimental

2.1. Functionalization of carbon nanotubes

Commercial MWNTs (Baytubes C 150-HP, Bayer Material Science AG, Germany) were functionalized using acid (concentrated nitric acid, 65%) and heating under reflux at 140 °C for 3 h as previously reported [16]. The f-CNTs were collected by centrifugation, re-dispersed in de-ionized water, washed thoroughly over a nylon membrane filter with pore sizes of 0.45 μm (Whatman, UK) during constant vacuum filtration until the filtrate turned neutral. Afterwards the f-CNT-cake was dried in a vacuum oven at 50 °C overnight. Finally, the resultant carbon cake was crushed, mixed and ground down into a fine powder using a mortar and pestle.

2.2. Functionalized buckypaper fabrication

The fBP fabrication was performed as reported in a previous work [16]. In short, 100 mg of f-CNTs were dispersed in 200 mL of an aqueous solution containing 1 wt.% Triton X-100 (Sigma Aldrich) under mechanical stirring for 30 min followed by ultrasonic bath treatment for 3 h. The resulting suspension was centrifuged for 15 min using a SIGMA 2-5 centrifuge at 2700 rpm to remove larger agglomerates of f-CNTs. The supernatant, containing a stable f-CNT-suspension, was then filtered through a nylon membrane filter and compressed under vacuum by an oil-free diaphragm pump (KNF Neuberger, Germany). The obtained homogenous black film was washed repeatedly with an excess of distilled water, followed by isopropyl alcohol and acetone. The prepared f-CNT-films were kept at room temperature for 30 min and then dried in a vacuum oven at 50 °C overnight.

2.3. Preparation BP-based biocathodes

The fBP-supported BOD catalysts were prepared according to the previous work. fBP pieces (3.0 mm diameter) were cut out of a 80 μm thick of free-standing fBP and glued onto a standard glassy carbon (GC) electrode tip using a conductive carbon paint (SPI). The GC was polished on alumina fine powder (0.3 μm) prior to every

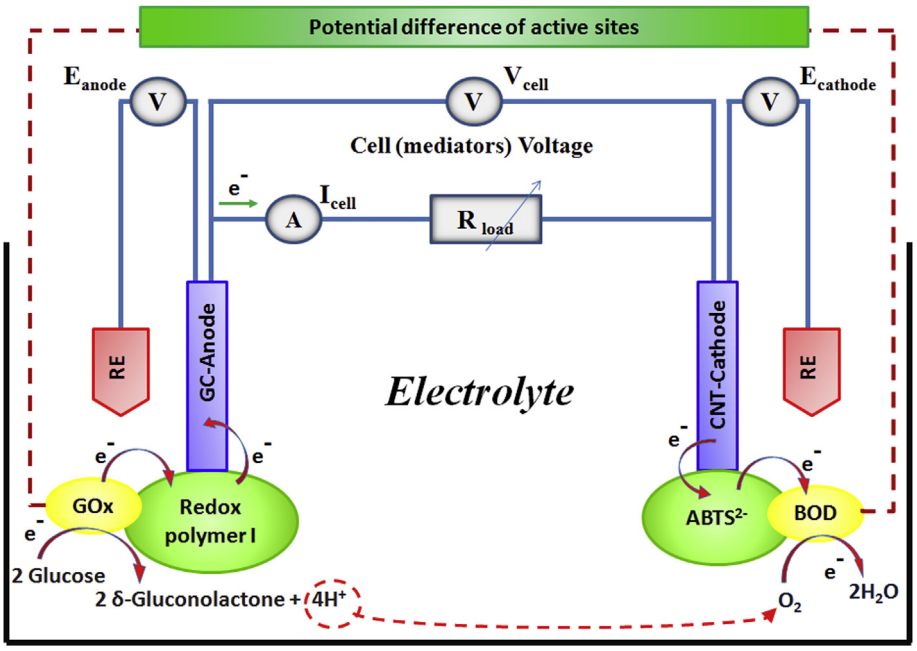

Fig. 1. Schematic configuration of the membraneless biofuel cell employing glucose and oxygen as a fuel and oxidizer, respectively.

measurement, rinsed with deionized Millipore-Q water (specific resistivity over 18.2 MΩ cm), ultrasonicated it for 1 min in water and then in ethanol, and finally dried before use. Bilirubin oxidase (BOD, Amano-3, [EC 1.3.3.5], activity 2.44 U mg^{-1}) from *M. verrucaria* was obtained from Amano Pharmaceutical Co. (Japan) and as ET mediator, 2,2′-azinobis(3-ethylbenzothiazoline-6-sulfonate) diammonium salt ($ABTS^{2-}$) from Sigma Aldrich was used.

Typically, the biocatalyst inks were prepared consisting of 3 mg of BOD, 12 vol.% Nafion solution (Nafion®, 5 wt.%, Sigma Aldrich) and 0.5 mM of $ABTS^{2-}$, in 0.1 M phosphate buffer solution (PBS) using deionized water. Afterwards, the resulting ink was pipetted directly onto the fBP to form BOD-$ABTS^{2-}$/fBP with a total enzyme loading of 175 μg cm^{-2}. The fBP-based electrodes were protected from dust, cured at room temperature for 2 h and then kept at 4 °C for at least 12 h. Finally, the electrodes were washed with deionized water and then stored in a PBS at 4 °C till use.

2.4. Preparation of ferrocene-based redox polymer bioanode

2.4.1. Material

N,N-Dimethylacrylamide, *N,N*-dimethylformamide (DMF) and triethylamine were dried with CaH_2 and distilled with reduced pressure. Methanol was dried using magnesium and iodine, and stored over activated molecular sieve (3 Å). All drying procedures were performed under nitrogen atmosphere and dried chemicals were stored and handled under nitrogen at all times. DMF was stored over activated molecular sieve (4 Å). All other chemicals were used as received. Glucose oxidase (GO_x) from *Aspergillus niger* with a specific activity of 148.4 ku g^{-1} was obtained from Sigma. 4-Methacryloyloxybenzophenone was synthesized from 4-hydroxybenzophenone and methacryloylchloride in the presence of triethylamine in a standard esterification reaction [33,35]. *N*-Methacryloyl-β-alanine succinimide ester was synthesized according to a reported procedure [33,36].

2.4.2. Preparation of the redox polymer

The redox polymer p(DMAA-8.5%MABP-10%FcOAm) was synthesized by preparation of an active ester pre-polymer and subsequent aminolysis. The general procedure has been published previously [31–33]. The amino linker that was utilized was 12-amino-6-aza-2-oxy-dodec-1-yl-ferrocene. It was synthesized from (ferrocenylmethyl) trimethylammonium iodide in three steps as described in Supporting Information.

2.4.3. Bioanodes preparation

A mixed solution of polymer and enzyme (25% GO_x, total mass concentration 75 mg mL^{-1}) was spin coated onto pre-polished glassy carbon electrodes (standard 3 mm diameter GC tips, *Radiometer Analytical*, Villeurbanne, France). Crosslinking and immobilization was simultaneously achieved by irradiation through a foil mask ($\lambda \geq 365$ nm, total irradiation dose of 80 J cm^{-2}) [31–33]. This step was repeated to increase the total loading with materials, and the electrodes were washed extensively water and stored in buffer before use.

2.5. Electrochemical experiments

Electrochemical experiments were conducted in a thermostated electrochemical cell in PBS (pH 7.2) at 37 °C. Glucose concentrations were obtained by adding aliquots of 1 M glucose solution, which had been allowed to mutarotate for at least 24 h. A platinum plate counter electrode and Ag/AgCl (3 M KCl) reference electrode (Metrohm, Filderstadt, Germany) were used, as well as an *EDI-101* rotating disk electrode holder (RDE) and a CTV-101 control unit (*Radiometer Analytical*, Villeurbanne, France) along with exchangeable GC tips. The voltammetric experiments of the electrodes were conducted with an Ivium Compactstat electrochemical analyzer controlled by the IviumSoft Electrochemistry Software [33,34].

2.6. Biofuel cell assembly and testing

The representation of our BFC is depicted in Fig. 1. All the measurements were carried out in a thermostated electrochemical cell (single compartment) at 37 °C, in a PBS (pH 7.2) buffer.

BFC tests were conducted in a potentiostatic mode using an Autolab PGSTAT-30 potentiostat/galvanostat (ECO Chemie B.V.,

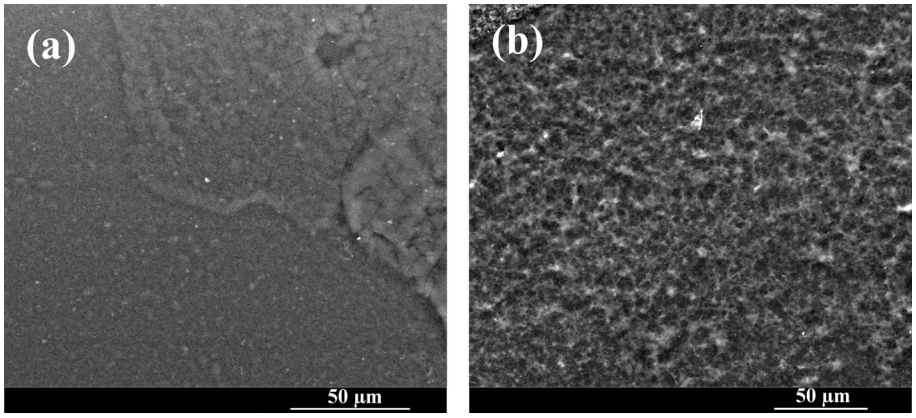

Fig. 2. SEM images of the surfaces of a) redox polymer-based bioanode, and b) fBP-based biocathode.

Netherlands) controlled by the GPES software. A bubbler was used and gases were pre-saturated with water by passage through it [33,34].

The cell potential was decreased from the open circuit voltage to zero cell voltage in steps between 25 mV and 75 mV. For each new applied potential, the current was measured for 5 min and the potentials of the individual electrodes were simultaneously recorded against reference electrodes (RE).

2.7. Physiochemical and morphological characterization

^{1}H NMR and ^{13}C NMR spectra were recorded on a Bruker 250 MHz instrument. GPC measurements were performed in DMF containing 3 g L^{-1} LiCl against a PMMA standard. The UV irradiation was carried out with an Oriel 69910 Arc Lamp from Newport, which was operated with an I-filter cutting off light with a wavelength below 365 nm.

The morphology of agglomerated MWNTs as well as BP-electrodes was investigated by scanning electron microscopy (SEM, Quanta 250 FEG, FEI, Oregon, USA).

Nitrogen adsorption/desorption isotherms were conducted at −196 °C on an automatic analyzer (Sorptomatic 1990, Porotec, GmbH). Prior to the experiment, the samples were degassed by heating at 250 °C for 5 h under high vacuum. The texture properties were analyzed using advanced data processing software (ADP version 5.1, Thermo Electron Corporation Milan, Italy).

The specific surface areas (given in m^2 g^{-1}) of fBP powder samples were evaluated from the linear part of the adsorption plot of N_2, according to the standard Brunauer–Emmett–Teller (BET) method, at a relative pressure range of 0.05–0.3 p/p^0. The mean diameter of mesopores (2–50 nm) was deduced from the desorption branch of the isotherm relative pressure in the range of 0.4–0.999 p/p^0 using a model developed by Barrett, Joyner and Halenda (BJH).

The electrical conductivity measurements of BPs were carried out on a four-point probe instrument (QuadPro resistivity system, Lucas Signatone) and the thicknesses of BPs were measured using a micrometer gauge (resolution 1 µm, Mitutoyo).

3. Results and discussion

3.1. Electrode morphology

The SEM images of fBP-based cathode and ferrocene-containing redox polymer-based bioanode are shown in Fig. 2. From these images, one can easily see the smooth surface of the bioanode. The fBP cathode, on the other hand, shows the highly porous structure. Following the BET and BJH-models one can calculate the specific surface areas of 279 m^2 g^{-1} and a median pore diameter of 54 nm for fBPs. This could facilitate a better mass transport within the fBP-based electrode for reactive species.

In summary, this indicates that the homogenous dispersion of nanotubes in fBP may allow enhanced BOD adsorption and reduce diffusional resistances.

In terms of electrical conductivity, fBP of 80 µm thick exhibits an apparent electrical conductivity of ca. 0.9 S cm^{-1}. This value is sufficient for the low current densities in BFCs and thus no additional current collector is needed in electrode fabrication. Moreover, by immobilization on the supporting membrane filter the fBP-electrodes exhibit excellent long-term mechanical stability in aqueous solution.

3.2. Variation of glucose concentration

3.2.1. Bioanodes

The anodes used in this study are based on the immobilization of the biocatalyst in a water-swellable polymer network with incorporated redox active moieties. This polymer network contains a large volume fraction of water and is therefore an ideal immobilization matrix for biological molecules [37]. If suitable mediator units are attached to the backbone of the polymers, they serve as a non-leachable electronic “wire” between the immobilized biocatalyst and the conductive support [27,28,38]. The polymer that was utilized in this study was designed on the basis of our previous publications [31,32].

Ferrocene (Fc) units were chosen as mediator moieties, as they are chemically stable, readily available, non-toxic [39], and undergo fast ET with glucose oxidase [17,18,40–42]. In order to enhance the mobility of the redox units, they were separated from the polymer backbone via long, flexible spacers [43]. The design of the spacer was carried out based on previous findings in our laboratory and the group of Schmidtke [31,32,44]. It was observed that polymers with a basic amino group in close proximity to the redox unit have a limited stability in the oxidized state in physiological buffer [31,32,44], presumably as the result of irreversible uptake of dibasic phosphate [31,33,45]. A stabilization is feasible if no (temporary) charges are present [32,33], or if the charges are spatially separated from the redox unit [45]. As completely uncharged polymers have a limited water solubility, and as microphase separation with the negatively charged biocatalyst has to be suspected, the polymer designed for this study contained amino groups, but not in the immediate proximity of the redox unit.

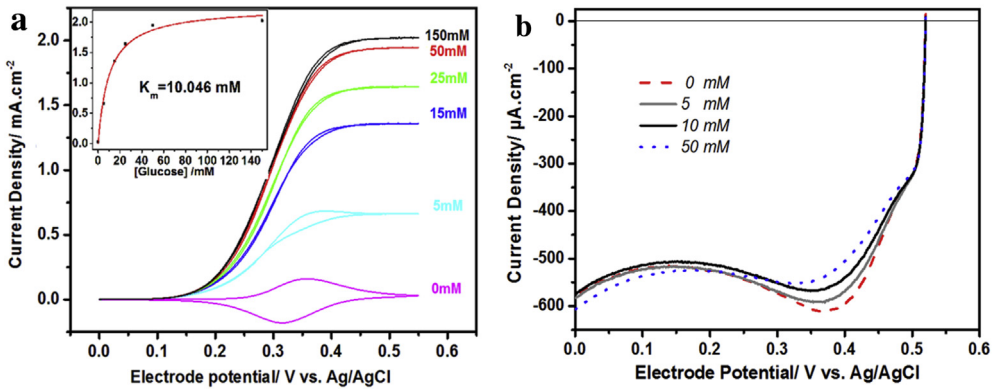

Fig. 3. a) Current responses of a typical bioanode depending on the glucose concentration measured using RDE at 1000 rpm, in Ar-purged PBS. The inset is the relationship between current generated and glucose concentration at 0.5 V, and the curve shows a Hill fit to experimental data, and b) The ORR curves of BP-based biocathode in different glucose concentrations in air-saturated PBS. Measurement conditions: potential scan rate 5 mV s^{-1}, pH 7.2, 37 °C.

According to UV–vis and ^{1}H NMR analysis, the polymer had the composition p(DMAA–7.9%MABP–9.6%FcOAm), which is within the experimental error of the monomer ratio (8.5% AMBP and 10% MAC_2AE). According to GPC analysis, the polymer had an M_w of 167,800 g mol^{-1}, M_n of 49,000 g mol^{-1}, corresponding to a polydispersity of 3.4.

A mixture of polymer and enzyme was deposited by repeated spin coating from solution containing 25 wt% GO_x and UV irradiation.

In the absence of the substrate (glucose), the reversible one-electron oxidation and reduction of the ferrocene mediator with a redox potential of about 340 mV *vs.* Ag/AgCl is observed (Fig. 3a). Upon addition of glucose, the shape of the cyclic voltammograms changes notably.

A strong catalytic oxidation current is observed and the reduction peak disappears as electrons are transferred from the FAD-cofactor of the enzyme to the conductive support through the electron-conductive matrix. No reduction peak or hysteresis is observed above 5 mM at the rotating electrode. Fig. 3a shows the typical current response of a modified anode rotating at 1000 rpm to the addition of glucose aliquots in argon-purged PBS. Hyperbolic Michaelis–Menten substrate saturation kinetics are observed. The current response was modeled for duplicate measurements at 6 different substrate concentrations using the Hill equation [46]. The fit yields a limiting catalytic current density of 2.2 mA cm^{-2} and an apparent Michaelis–Menten constant (K_m) of 10.0 mM.

The small value of K_m is better than values of similar materials and methods [24,44], indicating that the designed polymer possessed excellent ET and transport properties with high affinity to glucose. This is confirmed by the remarkably high catalytic current densities [44,45].

3.2.2. Biocathode

As can be seen in Fig. 3b, the BP-based biocathode shows no significant change of ORR catalytic current density in air-saturated PBS containing different glucose concentration up to 50 mM. This demonstrates clearly that this electrode can be effective under physiological conditions.

3.3. The influence of oxygen concentration

3.3.1. Bioanodes

The effect of oxygen, which is the natural electron acceptor of GO_x, on the catalytic current was studied in the presence of 15 mM glucose in PBS purged with argon, air or oxygen respectively (Fig. 4a).

Here, the anodic glucose electro-oxidation current decreases a little in the presence of oxygen because O_2 competes with the Fc-based redox polymer for the GO_x-$FADH_2$ electrons (Eqs. (4) and (5)):

$$\beta - d - glucose + GOx - FAD \rightarrow \delta - gluconolactone + GOx - FADH_2 \quad (1)$$

$$GOx - FADH_2 + 2Fc^+ \rightarrow GOx - FAD + 2Fc + 2H^+ \quad (2)$$

$$2Fc \rightarrow 2Fc^+ + 2e^- \quad (3)$$

$$GOx - FADH_2 + O_2 \rightarrow GOx - FAD + H_2O_2 \quad (4)$$

$$2H_2O_2 \rightarrow O_2 + 2H_2O + 2e^- \quad (5)$$

In an oxygen-purged buffer, the plateau current is only about 14% lower than in de-aerated PBS. It can thus be concluded that the glucose oxidation electrodes should be well suited for use as anodes in membraneless enzymatic BFCs, which need to operate in the presence of the oxidant.

3.3.2. Biocathodes

In the presence of O_2 in solution and ET mediator ($ABTS^{2-}$), BOD catalyzes the following reaction:

$$4ABTS^{2-} + 4H^+ + O_2 \rightarrow 4ABTS^{1-} + 2H_2O \quad (6)$$

The polarization curve of the biocathode (Fig. 4b) is obtained at 37 °C in PBS (pH 7.2) with O_2-saturated PBS. A catalytic electroreduction current corresponding to the indirect reduction of dioxygen to water appears at 0.53 V *vs.* Ag/AgCl and reaches a plateau at −700 µA cm^{-2} indicating that the reaction is controlled by diffusion. Besides, the shape of the polarization curve presents a peak at ca. 0.42 V, which could be explained by the direct reduction of $ABTS^{2-}$. The current density of oxygen electroreduction in O_2-saturated PBS, is higher than that in air-saturated PBS. This confirms that the influence of natural diffusion (mass transport) is a limiting factor.

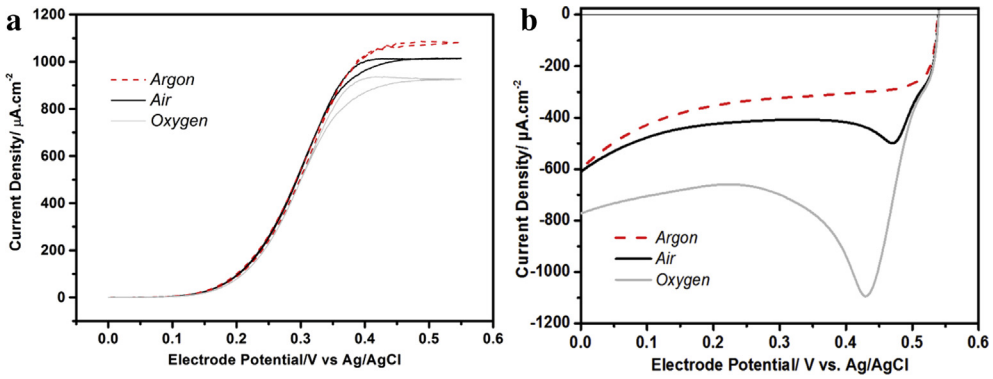

Fig. 4. a) Cyclic voltammograms for a typical anode rotating at 1000 rpm in the presence of 15 mM glucose, and b) The ORR curves of biocathodes in the presence of 5 mM glucose. Measurement conditions: potential scan rate 5 mV s^{-1}, PBS (pH 7.2), 37 °C, under different atmosphere.

3.4. Complete biofuel cell tests

3.4.1. Reproducibility

Fig. 5 shows the results of three independent experiments that were carried out in the presence of a physiological glucose concentration (5 mM) in air-saturated PBS.

It can be seen that the properties of both electrodes and, in consequence, of the complete BFC, were very well reproducible. The anodic open circuit potential (OCP) varied between −53 mV and −63 mV *vs.* Ag/AgCl, while the OCP of the cathodes amounted to values between 499 mV and 515 mV *vs.* Ag/AgCl. Accordingly, the open circuit voltage (V_{oc}) of the cell was obtained as (555 ± 11) mV. BFC produced an average of (15.8 ± 1.7) µW cm^{-2} at an operating voltage between 175 mV and 200 mV, and short circuit current densities (I_{sc}) of about 180 µA cm^{-2} were obtained. The values compare well to those reported recently for other BFCs (with 5 mM glucose) based on immobilized enzymes [47], but are still lower than those obtained with the osmium complexes by Mano's group for the membraneless enzymatic BFCs that generated 740 µ W cm^{-2} at 0.57 V, in physiological buffer containing 15 mM glucose [48].

The cell voltage shows an initial drop in the low current region and a steady decrease at higher currents. From the electrode polarization plots, overpotential contributions from the anode and the cathode are distinguishable. The potential of the anode follows a logarithmic trend and increases faster in the low current region that in the high current range. The cathode characteristics are quite different, with a strong potential drop in the high current density region and a stable trend at low currents.

It can be noted here that the activation polarization at the anode causes the initial drop of the BFC voltage while the cathode causes the late drop due to the diffusion polarization (mass transport limitation) at high current densities. The likely origin of this effect on the bioanode is the Nernstian control of the equilibrium ratio between the oxidized and the reduced form of the mediator. An equal concentration of both forms is present at the half-wave potential of about 340 mV *vs.* Ag/AgCl, at which charge transport is, accordingly, most rapid [38]. The OCP of the GO_x-containing anode in the presence of 5 mM glucose is lower by about 400 mV due to the reduction of the mediator by the enzyme. However, only negligible charge can be transported through the redox hydrogel matrix at this potential, and the electrode potential increases rapidly with increasing current until a more balanced ratio between the two oxidation states is obtained. Moreover, the potential drop at high current densities is most likely attributed to oxygen mass transport limitation on the cathode side.

3.4.2. The influence of glucose concentration

The effect of the concentration of glucose on the BFC was investigated for the concentrations range between 0 mM and 15 mM. The results are presented in Fig. 6.

Measurements that were carried out in air in the presence of 5 mM and 15 mM glucose showed a slightly enhanced cell performance at the higher substrate concentration. The slight shift of the anode potential to lower values does not significantly affect the overall cell characteristics, as the mass transport limitations of oxygen dominate the overall cell overpotential. No significant cell current was generated in the absence of the fuel, as expected.

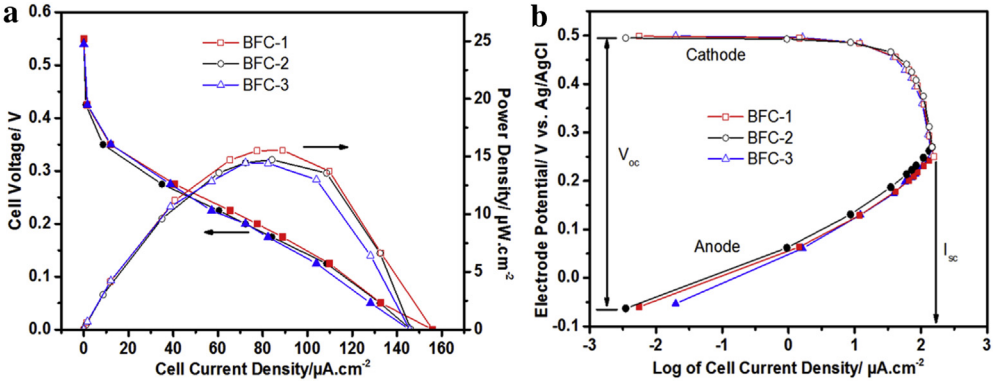

Fig. 5. a) Power output and cell voltage that were obtained in three independent fuel cell measurements on single use electrodes (air-saturated PBS, 5 mM glucose): solid symbols represent the cell voltages, and open symbols represent the cell power densities, and b) corresponding linear polarization curves of the electrodes: solid symbols represent the anode potentials, and open symbols represent cathode potentials.

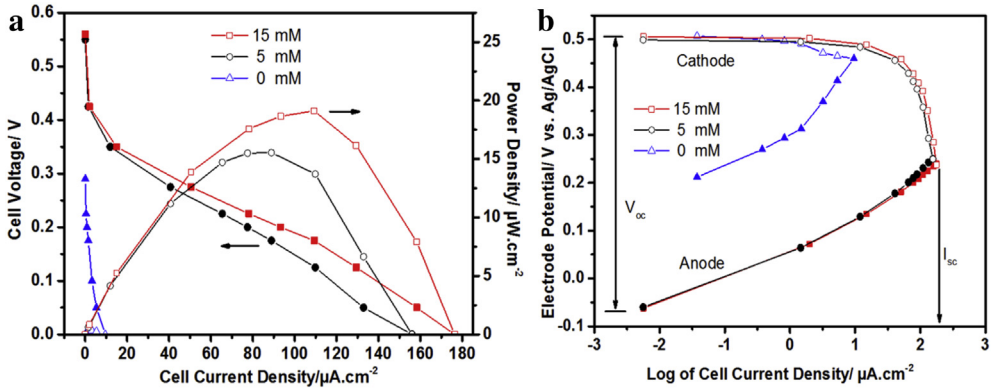

Fig. 6. a) Fuel cell power output and cell voltage in air-saturated PBS containing different glucose concentration: solid symbols represent the cell voltages, and open symbols represent the cell power densities, and b) corresponding linear polarization curves of the electrodes: solid symbols represent the anode potentials, and open symbols represent cathode potentials.

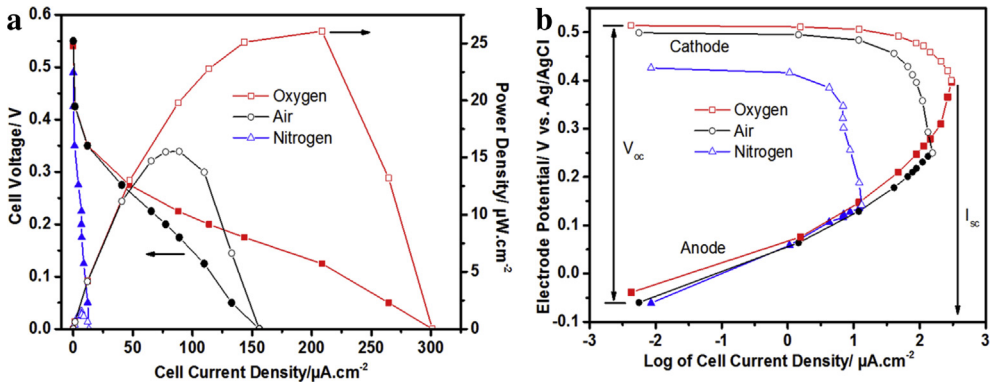

Fig. 7. a) Fuel cell power output and cell voltage in PBS containing 5 mM glucose saturated with oxygen, air and nitrogen atmospheres: solid symbols represent the cell voltages, and open symbols represent the cell power densities, and b) corresponding linear polarization curves of the electrodes: solid symbols represent the anode potentials, and open symbols represent cathode potentials.

3.4.3. The influence of oxygen concentration

If the concentration of the oxidant was increased by saturating the PBS with pure oxygen, the cathode potential suffered less from mass transport limitations (Fig. 7). A BFC power output of up to 26 μW cm^{-2} was obtained, while the short circuit current density (I_{sc}) increased to a value of 300 μA cm^{-2}. The anode polarization plot shows a slight shift to positive potentials due to the undesirable competition of dissolved oxygen and ferrocene to the electrons from GO_x, in agreement with the findings for the individual electrode (Fig. 4).

It may be noted that the concentration polarization of glucose to the anode begins to contribute significantly to the cell overpotential, as indicated by the higher slope of the *V–I* plot for the anode at current densities above 200 μA cm^{-2}. Moreover, undesirable electron transfer from GO_x-$FADH_2$ electrons (Eqs. (4) and (5)) to available oxygen in solution and formation of hydrogen peroxide might have a negative influence on the activity of enzyme. However, in contrast to the fact reported by Mano et al., the current result with ferrocene mediation seems to be more effective in O_2-saturated PBS [49]. The electrochemical activity of the individual electrodes was unaffected after BFC testing.

4. Conclusions

In this study the advances in polymer chemistry and nanotechnology have been merged, in order to develop membraneless, one-compartement glucose/O_2 enzymatic BFCs. This was obtained by using efficient mediated electron transfer bioelectrocatalytic systems. BFCs were successfully assembled in a highly reproducible manner and operated in physiological conditions. The cells were based on glucose-oxidizing anodes with glucose oxidase and ferrocene-containing redox polymer, and an oxygen-reducing cathode with bilirubin oxidase and highly conductive and mesoporous buckypaper, similar to our previously reported electrodes [16,30–32].

Using such three-dimensional electrodes based on redox hydrogel matrix or carbon nanotube entanglements (buckypaper) can improve enzyme loading and thus solve the problems associated with the use of traditional two-dimensional electrodes. The performance of the cells was studied depending on the operation conditions. The highest power output of 26 μW cm^{-2} at 0.20 V was achieved in oxygen-saturated solution with a physiological glucose concentration of 5 mM. This value compares very well to other recently published enzymatic BFCs [47], although the best membraneless enzymatic BFC based on osmium-redox polymer yields power density of 740 μW cm^{-2} at 0.57 V (with 15 mM glucose) [48]. Therefore some optimizations must be made in order to compete with this benchmark value.

The limitation of power density achieved with the BFC is mainly attributed to the low open circuit voltage compare to the thermodynamic value of 1.18 V [50], due to the relatively high anode overpotential resulted from the positive potential of ferrocene-containing polymer, and to the cathode overpotential at high current density. However, in contrast to the fact reported by Mano

et al. [49], our result with ferrocene mediation seems to be more effective in O_2-saturated PBS. The advantage of our approach is that no toxic substances like osmium are used. To support this tactic, other non-toxic mediators could be investigated in order to build effectively high power density BFCs.

Additionally, the redox potential of the ferrocene moiety can be lowered if substituents are added that increase the electron density of the complex. For example, dimethylferrocene moieties have been reported to have an up to ca. 90 mV lower redox potential than corresponding ferrocene units [42]. The current density could be improved if conductive nanomaterials such as CNTs were used.

Finally, the following approaches can be applied to enhance the membraneless BFC performance by: I) Hydrogen peroxide, which is most likely formed from the direct reaction of GO_x and oxygen, could be removed by adding catalase to the anodes. This might enhance cell performance, as H_2O_2 impairs the activity of the biocatalysts [51]. II) An oxygen-insensitive anode biocatalyst could be used instead of GO_x, e.g. a combination of pyranose dehydrogenase and cellobiose dehydrogenase can also yield four electrons from glucose oxidation upon oxidizing glucose molecule regioselectively [51]. III) An open-to-air approach for a gas diffusion cathode could be studied in order to reduce oxygen concentration polarization [52].

Acknowledgments

The authors are very grateful to the German Science Foundation (DFG) through the research training group (Graduiertenkolleg GRK 1322 “Micro Energy Harvesting”) for the financial support. Thanks are also due to Dr. Ralf Thomann for taking SEM images.

Appendix A. Supplementary data

Supplementary data related to this article can be found at http://dx.doi.org/10.1016/j.jpowsour.2013.08.077.

References

[1] A. Heller, AIChE J. 51 (2005) 1054–1066.
[2] H.-H. Kim, N. Mano, Y. Zhang, A. Heller, J. Electrochem. Soc. 150 (2003) A209–A213.
[3] A. Heller, Phys. Chem. Chem. Phys. 6 (2004) 209–216.
[4] A.T. Yahiro, S.M. Lee, D.O. Kimble, Biochim. Biophys. Acta (BBA) – Special. Sec. Biophys. Subj. 88 (1964), 375–283.
[5] A. Heller, B. Feldman, Chem. Rev. 108 (2008) 2482–2505.
[6] N.L. Akers, C.M. Moore, S.D. Minteer, Electrochim. Acta. 50 (2005) 2521–2525.
[7] M.J. Moehlenbrock, S.D. Minteer, Chem. Soc. Rev. 37 (2008) 1188–1196.
[8] J.A. Cracknell, K.A. Vincent, F.A. Armstrong, Chem. Rev. 108 (2008) 2439–2461.
[9] N.S. Lewis, D.G. Nocera, Proc. Nat. Acad. Sci. 103 (2006) 15729–15735.
[10] C.F. Blanford, C.E. Foster, R.S. Heath, F.A. Armstrong, Faraday. Discuss. 140 (2009) 319–335.
[11] V. Flexer, N. Brun, R. Backov, N. Mano, Energy Environ. Sci. 3 (2010) 1302–1306.
[12] E. Nazaruk, K. Sadowska, J.F. Biernat, J. Rogalski, G. Ginalska, R. Bilewicz, Anal. Bioanal. Chem. 398 (2010) 1651–1660.
[13] L. Hussein, S. Rubenwolf, F. von Stetten, G. Urban, R. Zengerle, M. Krueger, S. Kerzenmacher, Biosens. Bioelectron. 26 (2011) 4133–4138.
[14] D. Ivnitski, B. Branch, P. Atanassov, C. Apblett, Electrochem. Commun. 8 (2006) 1204–1210.
[15] O. Yehezkeli, Y.M. Yan, I. Baravik, R. Tel-Vered, I. Willner, Chem. Eur. J. 15 (2009) 2674–2679.
[16] L. Hussein, G. Urban, M. Kruger, Phys. Chem. Chem. Phys. 13 (2011) 5831–5839.
[17] N. Mano, V. Soukharev, A. Heller, J. Phys. Chem. B 110 (2006) 11180–11187.
[18] H.-z. Bu, S.R. Mikkelsen, A.M. English, Anal. Chem. 67 (1995) 4071–4076.
[19] G.T.R. Palmore, H.-H. Kim, J. Electroanal. Chem. 464 (1999) 110–117.
[20] A. Riklin, E. Katz, I. Wiliner, A. Stocker, A.F. Buckmann, Nature 376 (1995) 672–675.
[21] R. Szamocki, V. Flexer, L. Levin, F. Forchiasin, E.J. Calvo, Electrochim. Acta. 54 (2009) 1970–1977.
[22] J.W. Gallaway, S.A. Calabrese Barton, J. Electroanal. Chem. 626 (2009) 149–155.
[23] J. Gallaway, I. Wheeldon, R. Rincon, P. Atanassov, S. Banta, S.C. Barton, Biosens. Bioelectron. 23 (2008) 1229–1235.
[24] E.J. Calvo, R. Etchenique, C. Danilowicz, L. Diaz, Anal. Chem. 68 (1996) 4186–4193.
[25] I. Willner, V. Heleg-Shabtai, R. Blonder, E. Katz, G. Tao, A.F. Bückmann, A. Heller, J. Am. Chem. Soc. 118 (1996) 10321–10322.
[26] I.K. Willner, Eugenii, Angew. Chem. Int. Ed. 39 (2000) 1180–1218.
[27] B.A. Gregg, A. Heller, J. Phys. Chem. 95 (1991) 5976–5980.
[28] E. Katz, I. Willner, A.B. Kotlyar, J. Electroanal. Chem. 479 (1999) 64–68.
[29] T. Tamaki, T. Yamaguchi, Indus. Eng. Chem. Res. 45 (2006) 3050–3058.
[30] L. Hussein, Y.J. Feng, N. Alonso-Vante, G. Urban, M. Krüger, Electrochim. Acta. 56 (2011) 7659–7665.
[31] C. Bunte, O. Prucker, T. König, J. Rühe, Langmuir 26 (2010) 6019–6027.
[32] C. Bunte, J. Rühe, Macromol. Rapid Commun. 30 (2009) 1817–1822.
[33] C. Bunte, PhD Dissertation, Freiburg University, Germany, Der Andere Verlag, ISBN 978-3-86247-235-2, 2012.
[34] L. Hussein, PhD Dissertation, Freiburg University, Germany, 2012.
[35] R. Toomey, D. Freidank, J. Ruehe, Macromolecules 37 (2004) 882–887.
[36] H. Murata, O. Prucker, J. Ruehe, Macromolecules 40 (2007) 5497–5503.
[37] M. Moschallski, J. Baader, O. Prucker, J. Rühe, Anal. Chim. Acta. 671 (2010) 92–98.
[38] A. Heller, Curr. Opin. Chem. Biol. 10 (2006) 664–672.
[39] M.F.R. Fouda, M.M. Abd-Elzaher, R.A. Abdelsamaia, A.A. Labib, Appl. Organometal. Chem. 21 (2007) 613–625.
[40] A.E.G. Cass, G. Davis, M.J. Green, H.A.O. Hill, J. Electroanal. Chem. 190 (1985) 117–127.
[41] M.J. Green, H.A.O. Hill, J. Chem. Soc.-Faraday Trans. I 82 (1986) 1237–1243.
[42] A.E.G.D. . Cass, Graham, Graeme D. Francis, H.Allen 0O. Hill, W.J.H. Aston, I. John, Elliot V. Plotkin, Lesley D.L. Scott, Anthony P.F. Turner, Anal. Chem. 56 (1984) 667–671.
[43] N. Mano, J.L. Fernandez, Y. Kim, W. Shin, A.J. Bard, A. Heller, J. Am. Chem. Soc. 125 (2003) 15290–15291.
[44] S.A. Merchant, D.T. Glatzhofer, D.W. Schmidtke, Langmuir 23 (2007) 11295–11302.
[45] S.A. Merchant, M.T. Meredith, T.O. Tran, D.B. Brunski, M.B. Johnson, D.T. Glatzhofer, D.W. Schmidtke, J. Phys. Chem. C 114 (2010) 11627–11634.
[46] R. Murray, V. Rodwell, D. Bender, K.M. Botham, P.A. Weil, P.J. Kennelly, Harper's Illustrated Biochemistry, 28th ed., McGraw-Hill Companies Incorporated, 2009.
[47] O. Yehezkeli, R. Tel-Vered, S. Raichlin, I. Willner, ACS Nano. 5 (2011) 2385–2391.
[48] F. Gao, L. Viry, M. Maugey, P. Poulin, N. Mano, Nat. Commun. 1 (2) (2010) 1–7.
[49] N. Mano, F. Mao, A. Heller, J. Am. Chem. Soc. 125 (2003) 6588–6594.
[50] V. Soukharev, N. Mano, A. Heller, J. Am. Chem. Soc. 126 (2004) 8368–8369.
[51] M.N. Zafar, F. Tasca, S. Boland, M. Kujawa, I. Patel, C.K. Peterbauer, D. Leech, L. Gorton, Bioelectrochemistry 80 (2010) 38–42.
[52] A. Zebda, C. Gondran, A. Le Goff, M. Holzinger, P. Cinquin, S. Cosnier, Nat. Commun. 2 (2011) 1–6.